JOURNAL OF MATERIALS SCIENCE **35** (2000) 3659–3667

Crystallization of leucite as the main phase in aluminosilicate glass with low fluorine content

M. B. TOŠIĆ
Institute for Technology of Nuclear and other Mineral Raw Materials, 86 Franche d' Esperey, 11000 Belgrade, Yugoslavia
E-mail: m.tosic@itnms.ac.yu

M. M. MITROVIĆ
Faculty of Physics, University of Belgrade, 12-16 Studentski trg, 11000 Belgrade, Yugoslavia

R. Ž. DIMITRIJEVIĆ
Faculty of Mining and Geology, University of Belgrade, 7 Đušina, 11000 Belgrade, Yugoslavia

The paper presents the results of the study of aluminosilicate glass that contains 0.77 wt% of F^- anions. The results show that the critical size of glass particles at which the surface mechanism of crystallization changes to volume crystallization is in the vicinity of 0.075 mm in this glass. The temperature of the maximum nucleation rate was determined to be $T_n = 680^\circ C$, and it is higher than the transformation temperature T_g. At crystallization temperatures up to $T_c = 950^\circ C$, the crystal phase of leucite is formed, alone. Above this temperature, besides the main phase of leucite, two other phases, diopside and phlogopite appear. The activation energy of crystallization $E_a = 319 \pm 23$ kJ/mol was determined. The results also show that the activation energy does not depend on the crystallization mechanism in this glass. The value of the Avrami parameters is $n = 1.45$. Microstructural studies confirmed the fact that volume crystallization of leucite takes place in this glass. The leucite crystals grow in form of equiaxial dendrites with pronounced anisotropy along the direction ⟨001⟩. Kinetical and microstructural studies show that the process of leucite crystal growth occurs at the smooth atomic scale-faceted crystal/glass interfaces and that it is controlled by volume diffusion. During the isothermal heat treatment the structure of dendrites changes.

1. Introduction

The dominant process that determines the microstructure of glass-ceramics is nucleation [1]. Therefore, the conditions under which the process of nucleation is evolved are the most important for designing the glass-ceramics microstructure. The changes of the melt temperature and the energetic barrier to crystal nucleation have a strong influence on nucleation rate due to the exponential relation that exists between these parameters. The value of nucleation barrier is altered with the change of level of undercooling and the addition of suitable agents. Previous studies have shown that an efficient way for obtaining high quality glass-ceramics is the addition of selected nucleating agents [2], the role of which is very complex [3, 4]. Their influence is mostly attributed to the effect of cations or anions inserted in the system. Presence of nucleating agents in the glass system significantly changes the intensity of bonds in the glass structure as well other properties. Moreover, two nucleation mechanisms, i.e. surface and volume crystallization, often act concurrently, which makes the glass crystallization a very complex process. As a result of using nucleating agent, the change of the glass crystallization mechanism from surface to volume crystallization takes place. Due to these reasons the choice of the kind and quantity of nucleator is not simple and it requires a detailed study.

Leucite ($KAlSi_2O_6$) is a framework pseudotetragonal aluminosilicate. Its structure consists of corner-linked $(Al,Si)O_4$ tetrahedra filled with K^+ cations [5]. It exhibits an interesting reversible phase transition in the temperature range 620–690°C [6]. At room temperature the leucite has a tetragonal symmetry and at high temperatures the structure becomes cubic. Its presence facilitates good mechanical, electrical and other properties suitable for various applications. Due to that, kinetics and mechanism of its crystallization are the subject of constant interest. The phase formation of leucite in the ternary SiO_2-Al_2O_3-K_2O system is very complex [2, 7]. The majority of glasses from the SiO_2-Al_2O_3-K_2O system crystallize by surface mechanism. Addition of nucleating agents such as TiO_2 or CeO_2 to these glasses causes change of their crystallization mechanism from surface to volume crystallization. Although it is difficult to establish the exact effect of these agents

on leucite nucleation, it is certain that TiO_2 and CeO_2 must be contained in the base glass [8].

The sample chosen for this study is a glass from the complex system SiO_2-Al_2O_3-CaO-MgO-K_2O with initial composition: $50{,}5SiO_2{\cdot}18{,}5Al_2O_3{\cdot}10{,}5CaO{\cdot}10{,}5MgO{\cdot}10K_2O$ (wt%). This composition was doped by CaF_2 in such quantity which makes the content of anion F^- in the glass to be 1 wt%. Fluorides as nucleation agents support phase separation, which indirectly affects the creation of nuclei [9]. For the additional quantity of CaF_2 the amount of CaO was reduced, so that the content of ions Ca^{2+} remained unchanged. The nucleation and crystallization study was performed at isothermal and non-isothermal conditions.

2. Experimental

Initial materials for obtaining the glass were quartz, Al_2O_3, MgO, CaO; CaF_2 and K_2CO_3, analytical grade. Preparation of the glass was performed in an electrical furnace in Pt crucible at $T = 1500^\circ$C for $t = 60$ min. The molten glass was cast on a metal plate and quenched in air. The obtained glass samples were transparent and without residual glass bubbles.

DTA investigations were carried out in a Netzch STA 409 EP device. Powdered Al_2O_3 was used as the reference material. For establishing the dominant crystallization mechanism the following powder samples were prepared with granulation: <0.038; 0.038–0.050; 0.050–0.1; 0.1–0.2; 0.2–0.3; 0.3–0.4; 0.4–0.5; 0.5–0.7 and 0.8–1 mm. The rate of heating was $v = 10^\circ$C/min, and the quantity of the studied sample was 100 mg.

The study of nucleation was carried out using powder samples with 0.5–0.7 mm granulation. The samples were heated at $v = 10^\circ$C/min rate up to the following temperatures: 600, 650, 660, 680, 685, 690, 700 and 710°C, at which temperatures they were kept for $t = 180$ min and then further heated to $T = 1100^\circ$C at the same heating rate.

Establishment of kinetic parameters of crystallization was carried out on the samples with the following granulation: <0.038 mm and 0.5–0.7 mm at the following heating rates: 2.5; 5; 7; 10; 15 and 20°C/min.

The second group of experiments was performed on compact glass samples. The experiments were performed in electric furnace with an automatic regulator that maintained the temperature with an accuracy of ±2°C. These samples were treated isothermally in two steps at $T_n = 680^\circ$C for $t = 180$ and 1200 min and then heated at the heating rate of $v = 2^\circ$C/min to $T_c = 900$; 950 and 1000°C at which they were kept for different times $t = 15$; 30; 60 and 180 min.

Dilatometric measurements were performed on samples with dimensions: diameter 3 mm, length 40 mm at the heating rate of $v = 10^\circ$C/min in the temperature range $T = 20$–900°C. Prior to measurement the sample was heated at $T = 700^\circ$C for $t = 20$ min.

The phase composition of the samples investigated was determined by using the X-ray powder diffraction (XRD) method. The powder patterns were obtained on a Philips, PW-1710 automated diffractometer, using a Cu tube operated at 40 kV and 35 mA. The instrument was equipped with diffracted beam curved graphite monochromator and Xe-filled proportional counter. Diffraction data were collected in the range 2θ, 4–70°, and 4–120°, counting for 0.25 and 10 seconds at 0.02 steps, respectively. A fixed 1° divergence and 0.1 receiving slits were used. The powders were mounted in a back-loaded sample holder using side-loading technique to avoid preference orientation of crystallites. The conditions for the scan were room temperature and ambient atmosphere. Powdered Si-standard reference material was used to correct the inter planar spacing for systematic errors. All reflections were profile fitted using a Pearson-VII function to obtain the accurate peak top locations. The quantitative portions of crystalline phase in the glass-ceramic were determined by full profile matching mode of Rietveld [10] refinement technique, by using the program Fullprof [11]. The published structural data for the determined minerals were used as starting parameters for the initial refinement.

Investigations of the crystal morphology were carried out using scanning electron microscopy SEM JSM 840 A Jeol. The samples were gold sputtered in a Jeol JFC 1100 ion sputter.

3. Results and discussion

3.1. The chemical composition of glass

The results of the chemical analysis indicate the following chemical composition of the obtained glass: $50.29SiO_2{\cdot}18.85Al_2O_3{\cdot}9.06CaO{\cdot}1.59CaF_2{\cdot}9.94MgO{\cdot}0.11Na_2O{\cdot}9.46K_2O$ (wt%). This glass contains 0.77 wt% of F^- anions. It is easily observable that the composition of the glass does not correspond with the stoichiometric composition of leucite. It contains 78.6 wt% of components necessary for the constitution of leucite.

3.2. Determination of dominant mechanisms of crystallization

Determination of the dominant crystallization mechanism (surface or volume) by which this glass is being crystallized was carried out according to the method suggested by C. S. Ray *et al.* [12]. According to this method, on the basis of DTA measurements either $(\delta T)_p$ or $T_p^2/(\Delta T)_p$ is plotted as a function of particle size, where $(\delta T)_p$ is the maximum height of the DTA peak, T_p is the temperature at $(\delta T)_p$ and $(\Delta T)_p$ is the width at the half peak maximum. As $(\delta T)_p$ is proportional to the total number of nuclei (volume and surface nuclei) contained in the glass [13] and $T_p^2/(\Delta T)_p$ is related to the crystal growth dimension [14], both of these values depend on the specific mechanism of crystallization.

For resolving of the dominant mechanism of crystallization, DTA curves were recorded at heating rate $v = 10^\circ$C/min on the samples with granulation of <0.038 to 1 mm. The recorded DTA curves show the exothermal peak at a temperature in the range $T_p = 901{,}4$–$962{,}8^\circ$C. Fig. 1 presents the DTA curves recorded on the samples with the smallest and the biggest granulation. The sample with the smallest

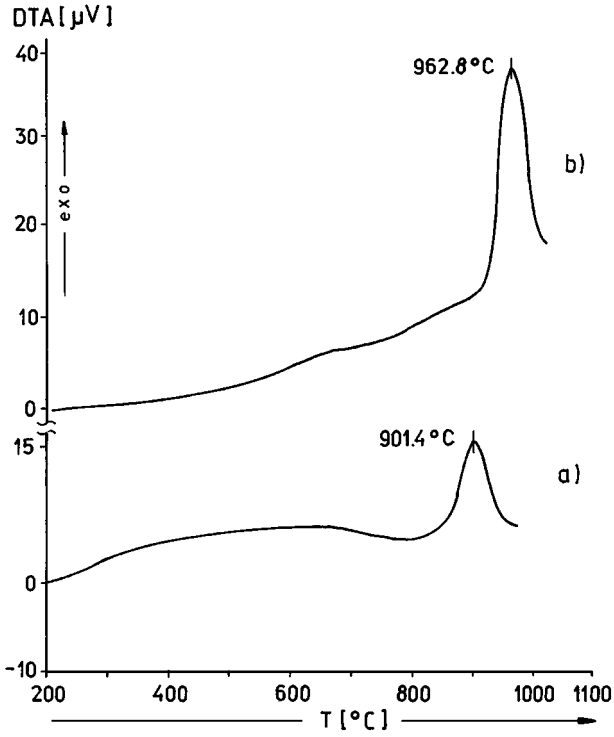

Figure 1 DTA traces recorded with heating rate 10°C/min: a) sample particle size <0.038 mm and b) sample particle size 0.8–1 mm.

granulation (curve 1a) displays the widest crystallization peak and the lowest temperature of the peak and *vice versa*.

Fig. 2a presents dependencies of $(\delta T)_p$ and $T_p^2/(\Delta T)_p$ on the mean value of the glass particles sizes. It is clear that the obtained curves display similar shapes on which three different areas can be seen. At the beginning, with the increase of the particle sizes, the value of $(\delta T)_p$ decreases until the dimension 0.075 mm. Behavior of the value $T_p^2/(\Delta T)_p$ in this region is complex. In the region around 0.075 mm the minimum appear, and with further increase of particle sizes (>0.075 mm) both values increase. Such curves suggest that at to particle sizes around 0.075 mm, the change in the mechanism of crystallization from surface towards volume glass crystallization occurs.

In the range of the smallest granulations (<0.075 mm), in the total number of present nuclei, the number of surface with respect to internal nuclei is dominant Due to that, the surface crystallization is dominant in these particles. With the increase of particle sizes, the ratio of surface to volume nuclei decreases, which results in decrease of the total number of nuclei, as well as the value $(\delta T)_p$ which is proportional to total number of nuclei. The variable $T_p^2/(\Delta T)_p$ should have a constant value for the dominant surface nucleation. In this case, the measurements were performed for just two particle sizes (0,019 mm and 0,045 mm), and similar values were arrived at for $T_p^2/(\Delta T)_p$. This is still insufficient for a reliable conclusion. However, the results in Section 3.5 also point to such behavior of $T_p^2/(\Delta T)_p$. They show that the activation energy for crystallization E_a in this glass does not depend on particle sizes, that is, on the mechanism of crystallization. Consequently, in case of granulation

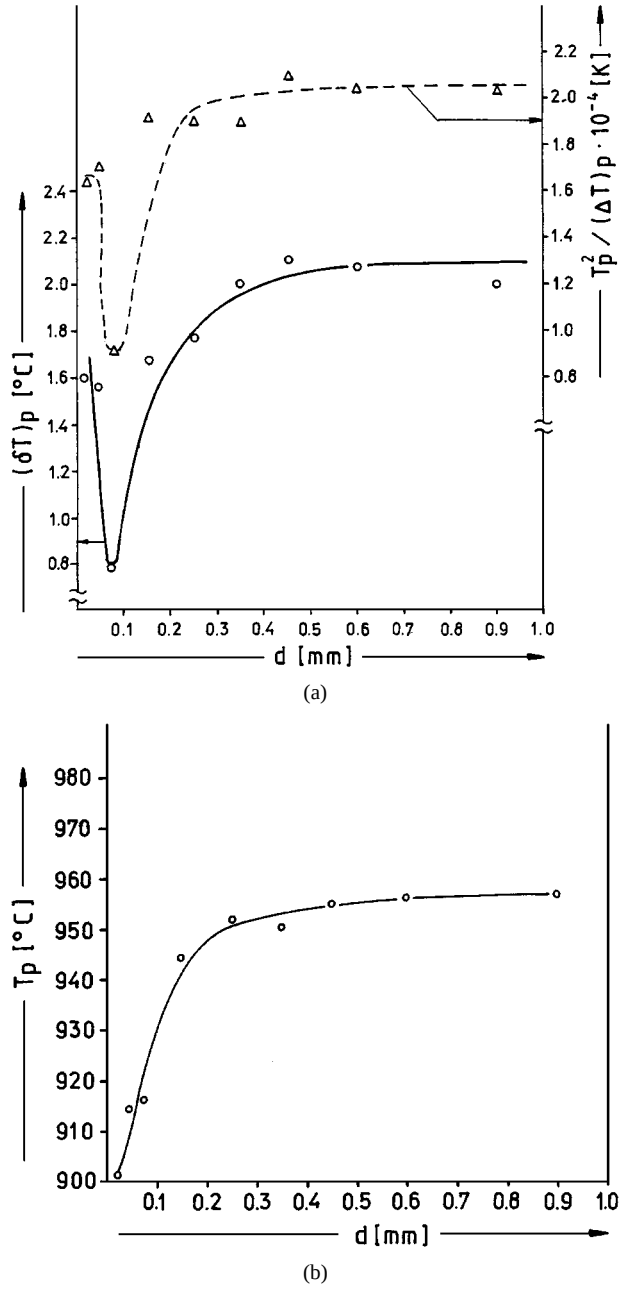

Figure 2 a) $(\delta T)_p$ and $T_p^2/(\Delta T)_p$ as a function of particle size and b) T_p as a function of particle size. DTA is heating rate, 10°C/min; sample weight, 100 mg.

<0.075 mm, the value $T_p^2/(\Delta T)_p$ should have a constant value $[T_p^2/(\Delta T)_p = 0.5E_a/2.5R = 7576]$.

In the range of glass particle sizes around 0.075 mm, the number of surface nuclei is reduced to such an extent that it is equalized with the number of volume nuclei. The total number of the present nuclei is the smallest and the values $(\delta T)_p$ and $T_p^2/(\Delta T)_p$ display minima.

The results of SEM investigations in Section 3.6 have shown that compact samples (of large sizes) are crystallized by the volume crystallization mechanism (Figs 7 and 8). Since with the increase of particle sizes the ratio of volume to surface grows as well, the number of internal nuclei increases with respect to the number of surface nuclei. Due to that, in the range of particle sizes >0.075 mm, the total number of nuclei increases too, as well as the values $(\delta T)_p$ and $T_p^2/(\Delta T)_p$.

Fig. 2b presents the dependence of the temperature of crystallization peak (T_p) from particle sizes. It is evident that T_p increases with the increase of particle sizes. However, such result indicates just the fact that, with the increase of particle sizes, the resistance to crystallization increases as well, although it is not possible to distinguish surface from volume crystallization from such behavior.

3.3. X-ray powder diffraction analysis

Samples used for XRD characterization were compact glass. These were subjected to heat treatment at isothermal conditions in two steps. The XRD results show that, on crystallization temperatures up to 950°C, only the leucite phase is distinguished in quantities proportional to the change of crystallization period. Summarized results of the XRD investigations are presented in Fig. 3. Curve a, presents the powder pattern of initial glass. Curves b–d coincide with samples crystallized at $T = 950$°C for times $t = 15$, 30 and 60 min. On the sample crystallized in the period $t = 60$ min (curve d), besides the well-crystallized leucite phase the traces corresponding to the diopside ($CaMgSi_2O_6$) pattern are recognized. On crystallization temperatures above 950°C, besides the two mentioned crystal phases, the phlogopite phase appears as well. Curve e represents the sample treated at 1000°C for 180 min. On this pattern, besides the crystallized leucite and diopside, the phlogopite phase is identified. Quantitative fractions of these phases were obtained from Rietveld XRD analysis, as shown in Table I and Fig. 4. The obtained results show that the investigated glass crystallized in three component glass-ceramic system with dominant leucite phase. Calculated unit cell dimensions were compared with literature data and no divergence was noticed. Moreover, the obtained cell dimensions for the phyllosilicate phase confirmed the 1M-polytype fluor-phlogpite phase, which is consistent with the initial mass balance.

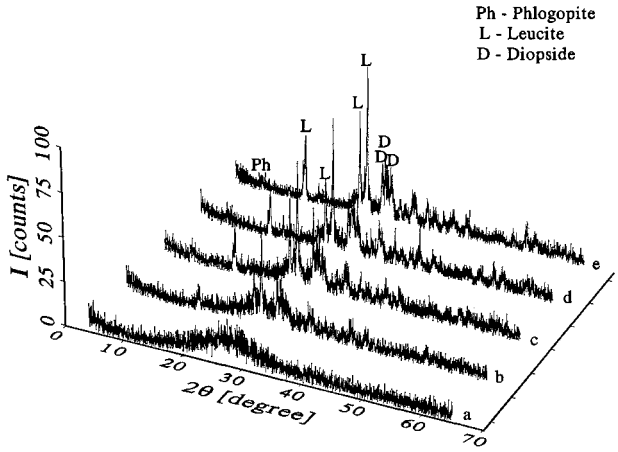

Figure 3 XRD patterns of: a) initial glass, b–d) crystallized glass with $T_c = 950$°C for $t = 15$, 30 and 60 min and e) crystallized glass with $T_c = 1000$°C for $t = 180$ min. All samples were nucleated at $T_n = 680$°C for $t = 1200$ min.

3.4. Nucleation behavior

Investigation of nucleation was carried out by the method based on DTA measurements, as suggested by Marotta *et al.* [13] and Ray and Day [14]. The following conditions have to be fulfilled for the application of this method: a) nuclei should not be formed during non-isothermal heating in the DTA experiment and b) bulk nucleation should occur in the glass. The results in Section 3.5 indicated that crystallization of this glass evolves at temperatures $T > 850$°C. On the other hand, previous investigations of nucleation in glass showed that it appears around the temperature of glass transformation (T_g) [15]. Dilatometric measurement of this glass sample revealed that the temperature of transformation is $T_g = 671$°C. These results demonstrate that nucleation and growth of crystal in this glass evolve in temperature ranges that differ by more than 150°C, therefore, the corresponding choice of heating rate during the DTA experiment facilitates satisfaction of condition (a) above. The heating rate chosen for these investigations was $v = 10$°C/min. In addition to that, the results in Section 3.2 demonstrate that volume crystallization within this glass appears with particle sizes >0,075 mm. Accordingly, for these experiments, glass powder whose particle sizes were 0,5–0,7 mm was chosen, which satisfies condition mentioned above (b). Theoretical deliberations [16] have shown that under these conditions, and the assumption that crystal growth follows during DTA a normal or screw dislocation growth mechanism, there is a linear relationship between the logarithm of the number of nuclei per unit volume N and the reciprocal value of the temperature of the crystallization peak ($1/T_p$):

$$\ln(N) = \frac{E_a}{RT_p} + \ln v + \text{const.} \qquad (1)$$

where v is the heating rate, E_a is the energy of activation of crystal growth and R is the gas constant. According to Equation 1, an increase in concentration of nuclei causes a shift of the peak towards lower temperatures and *vice versa*. This makes possible to obtain from the ratio $1/T_p$ to T a curve similar to the nucleation rate

TABLE I The most important crystallographic parameters for crystalline phases, of the present materials, obtained from Rietveld refinement of XRD pattern

Phase	Unit cell dimensions				Reliability factors		Quantitative volume fraction (%)
	a_0 (Å)	b_0 (Å)	c_0 (Å)	β (°)	Rb (%)	Rf (%)	
Leucite	13.1037 (3)	13.1037 (3)	13.7417 (3)	90.0	3.51	1.55	58
Diopside	9.7418 (5)	8.9022 (2)	5.2590 (3)	105.778 (3)	4.27	1.53	24
Phlogopite	5.3088 (3)	9.2015 (5)	10.1300 (5)	100.624 (3)	3.48	1.47	18

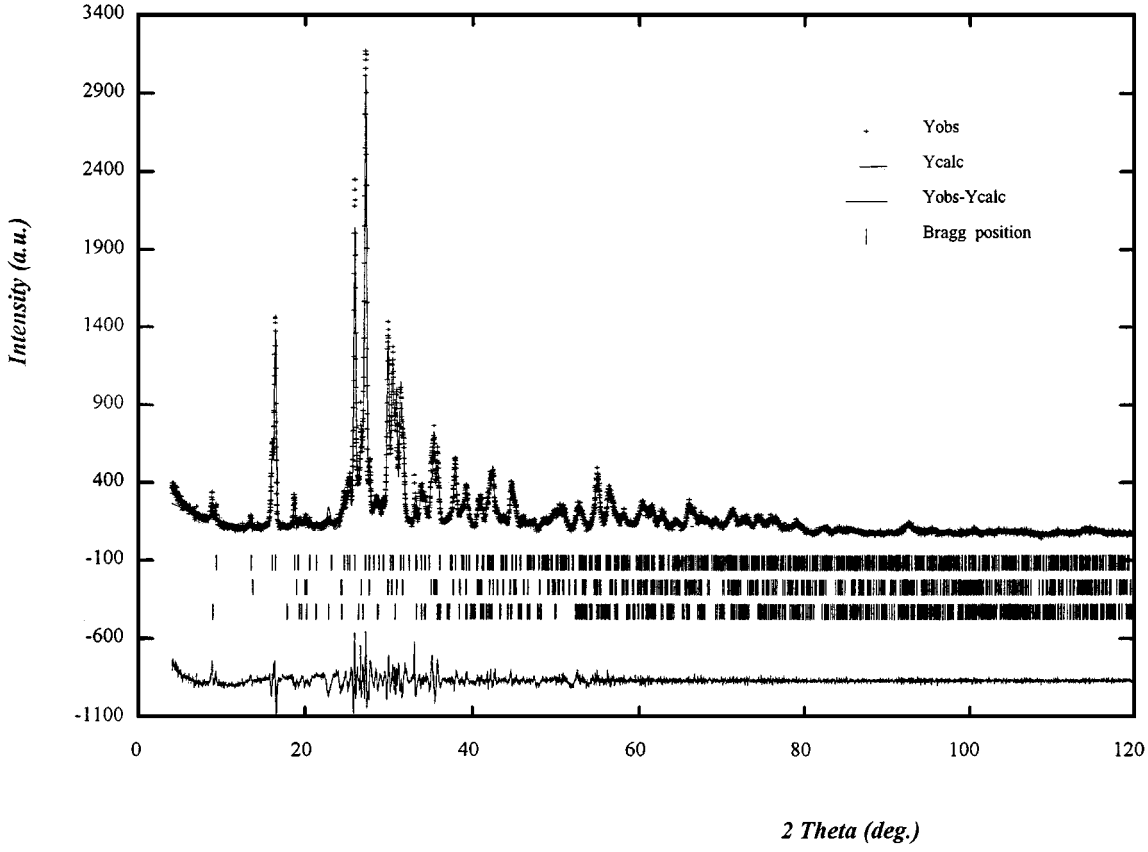

Figure 4 Rietveld refinement plot of glass sample treated at: $T_n = 680^\circ$C for $t = 1200$ min and $T_c = 1000^\circ$C for $t = 180$ min.

curve from which the temperature of the maximum nucleation rate T_n is determined.

SEM investigations (Section 3.6) show that leucite crystals grow in form of equiaxed dendrites with pronounced anisotropy. Previous investigations of crystal growth mechanism in glass have shown that, at high overcooling with pronounced anisotropy, the crystals grow by screw dislocation mechanism [17]. This discussion indicates that leucite crystal growth in this glass evolves on faceted interfaces by screw dislocation growth mechanism, which satisfies all required conditions for implementation of the Equation (1).

Fig. 5 presents the obtained dependence of $1/T_p$ from temperature. It is evident from Fig. 5 that, in the temperature region $T = 600$–710°C, an asymmetric curve was obtained, similar to the nucleation rate curve with maximum in temperature of 680°C. This is the temperature of the maximum nucleation rate (T_n). The value of T_n lies above the transformation temperature T_g. Previous investigations of glass nucleation have shown that, in case of volume nucleation, $T_n \geq T_g$ [15]. Therefore, the determined value of T_n indicates the temperature for volume nucleation in this glass.

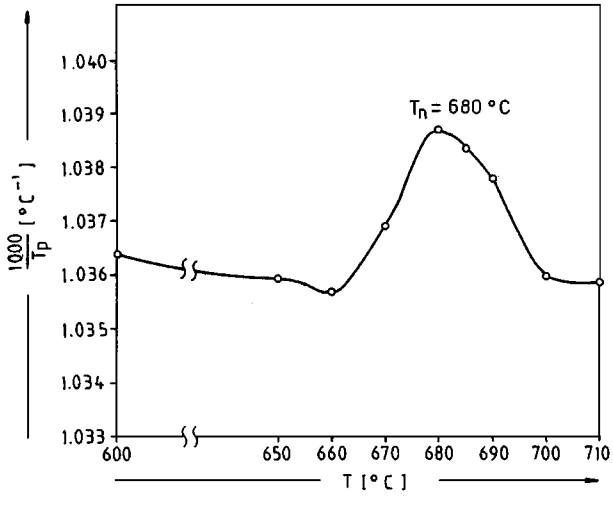

Figure 5 Dependence $1/T_p$ as a function of nucleating temperature.

The results of the XRD investigation have shown that, in case of samples subjected to heat treatment above 950°C, diopside and phlogopite appear as secondary phases. However, on the recorded DTA curve in the temperature region $T = 600$–710°C only one maximum appears at $T = 680^\circ$C. The reason for such result is probably a small number of developed crystals of secondary phases, what would explain why their appearance during DTA experiment has not been precisely registered. A small number of crystals in these phases can appear due to: (a) present significant induction time of nucleation or (b) nucleation rate of diopside and phlogopite is small in the temperature range $T = 600$–710°C. The result that $T_n \geq T_g$ indicates that this glass has a small induction time of nucleation, therefore, condition (a) is not followed. Data on nucleation of diopside and phlogopite for the glass of such composition are not available, therefore, condition (b) can be considered. The nucleation mechanism of this glass is very interesting as well as the question about the role of the present F^- ion included as nucleating agent. It is very probable that F^- ion, due to its strong weakening effect on the glass network, makes possible

easy atomic rearrangement, which, in turn, facilitates nucleation of leucite. The appearance of phlogopite is certainly related to the presence of fluorides. However, their number is small due to a insufficient concentration of F^- ion. The results of these investigations do not give sufficient evidence for establishing the nucleation mechanism. However, they clearly demonstrate that, in the presence of F^- anion (in the quantity of 0.77 wt%), this glass displays volume crystallization.

3.5. Crystallization kinetics

Analysis of the crystallization kinetics has been carried out on the basis of DTA measurements. Calculation of kinetic parameters was based on the modified form of the Kissinger equation, which has been proposed by Matusita *et al.* [18, 19]:

$$\ln\left(\frac{v^n}{T_p^2}\right) = -\frac{mE_a}{RT_p} + \text{const} \qquad (2)$$

where n is a constant known as the Avrami parameter and m represents the dimensionality of crystal growth. Factors n and m depend on the crystallization mechanism, and E_a values may be obtained from plots of ln (v^n/T_p^2) versus $1/T_p$, using the appropriate values of n and m. Analyses in Sections 3.2 and 3.4 have shown that in glass powder with particle sizes 500–700 μm, during DTA runs, the bulk crystallization evolves on constant number of nuclei. In this case the ratio between the parameters n and m is the following: $n = m$, that is, $E_a = E_{ak}$, where E_{ak} is the activation energy of crystal growth determined by Kissinger method. Table II presents temperatures T_p recorded at different heating rates for this sample. By using the Kissinger equation yields the value for the activation energy of crystal growth $E_a = 318 \pm 20$ kJ/mol, line A on Fig.6. Knowledge of the value of the parameter n is interesting as it points to the mechanism of crystal growth. Determination of the parameter n has been performed according to Ozawa method [20] from the following relation:

$$\ln[-\ln(1-x)] = n \cdot \ln[K(T_0 - T)] - n \cdot \ln v \qquad (3)$$

where T_0 denotes the starting temperature, T and x is temperature and volume fraction crystallized after time t, respectively. The Ozawa method is simple and straightforward, but in this case it is not possible to obtain more than three values of x, at the same temperature, for different rates, because the position of the

TABLE II The shift of crystallization peaks with different heating rates for powdered glass particles <0.038 and 0.5–0.7 mm

Heating rate [°C/min]	Particle size <0.038 mm T_p [°C]	Particle size 0.5–0.7 mm T_p [°C]
2.5	862	914
5	887.4	940
7	892.4	948
10	901.4	958.8
15	921.2	—
20	—	992.2

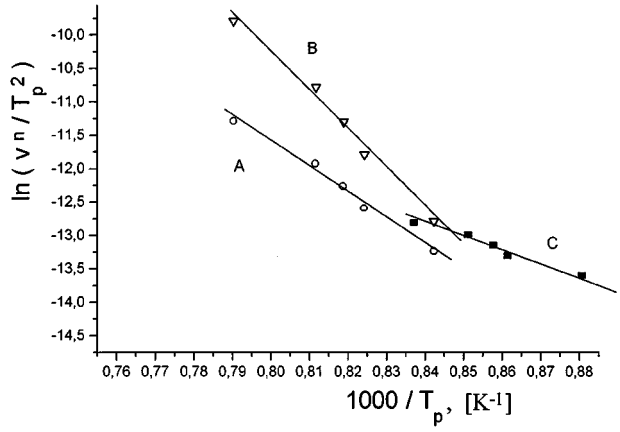

Figure 6 The plot of ln (v^n/T_p^2) versus $1/T_p$ for: A) sample particle size 0.5–0.7 mm ($n = 1$), B) sample particle size 0.5–0.7 mm ($n = 1{,}45$) and C) sample particle size <0.038 mm ($n = 0.5$).

crystallization peak shifts to higher temperature with increasing heating rates. Used for this calculation were the DTA curves recorded at heating rates $v = 2.5$, 5 and 7°C/min, at which crystallization peaks in the range 914–948°C were registered. The selected temperature was $T = 940$°C. The values of x were determined from the relation $x = S/S_0$, where S denotes the peak surface at a selected temperature and S_0 points to the total surface of the corresponding peak. The calculated value is $n = 1.45 \pm 0.15$. This value is close to $n = 1.5$ which is characteristic for three-dimensional crystal growth controlled by diffusion at constant number of nuclei [21]. However, the results of SEM investigations in Section 3.6 have shown that leucite crystals appear almost as two-dimensional dendrites. In this case the transformation takes place in a thin layer, meaning that the average dimension of the transformed area is considerably larger than the thickness of the layer. Consequently, the growth of crystal is generally two-dimensional. Such crystal growth, in case controlled by diffusion, coincides with the theoretical value of the parameter $n = 1$. Taking into consideration the experimental errors, the determined value $n = 1.45$ is still high. The probable reason for this is the presence of secondary phases whose mechanisms of crystal growth differ from the mechanism of leucite crystal growth, in spite of the fact that they were not registered at temperatures $T < 950$°C. The calculated value of E_a with coefficient $n = 1.45$ according to Equation 2, line B on Fig. 6, is $E_a = 324 \pm 20$ kJ/mol.

Table II presents temperatures T_p recorded at different heating rates on the sample with the smallest granulation, with particle size being <0.038 mm. Analyses in Section 3.2 have shown that, in case of this sample, the surface crystallization is dominant. In this case the value of n parameter is 0.5. On the basis of these results, and by using the value of $n = 0.5$ according to Equation 2 the calculated value of E_a is: $E_a = 315 \pm 30$ kJ/mol, (line C on Fig. 6). These results show that the values of E_a in both samples differ only within experimental and calculation error, and its mean value is $E_a = 319 \pm 23$ kJ/mol. This means that, in this case, E_a does not manifest dependence on particle sizes, that is, on crystallization mechanism. Under this condition the

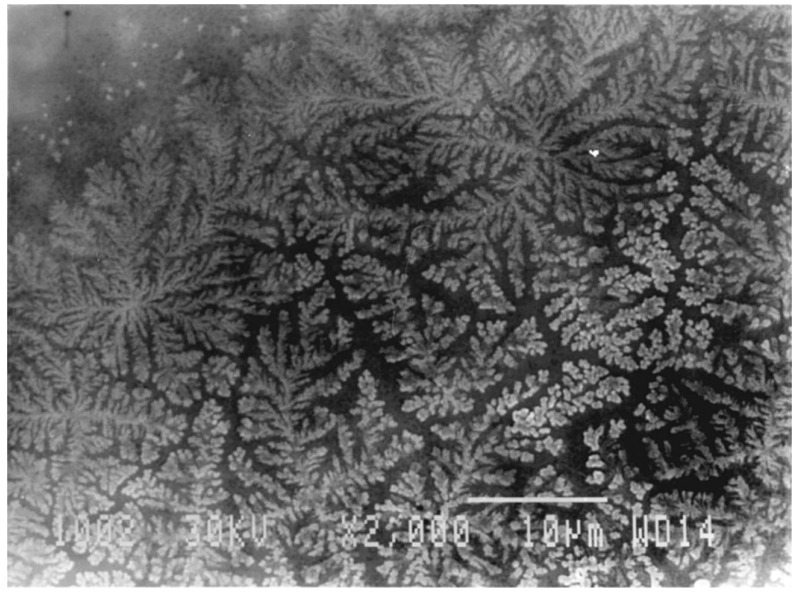

Figure 7 SEM micrographs for sample with heat treatment: $T_n = 680^\circ$C for $t = 1200$ min and $T_c = 950^\circ$C for $t = 30$ min.

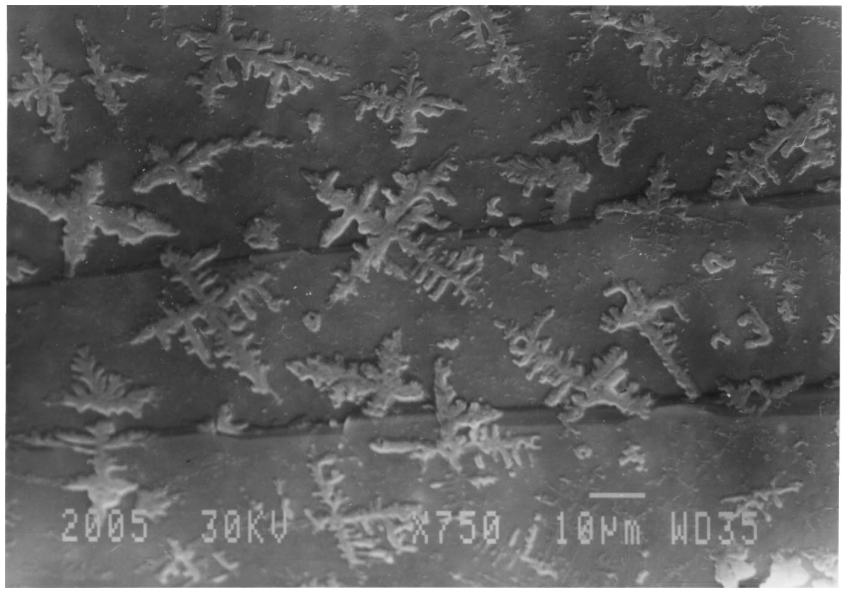

(a)

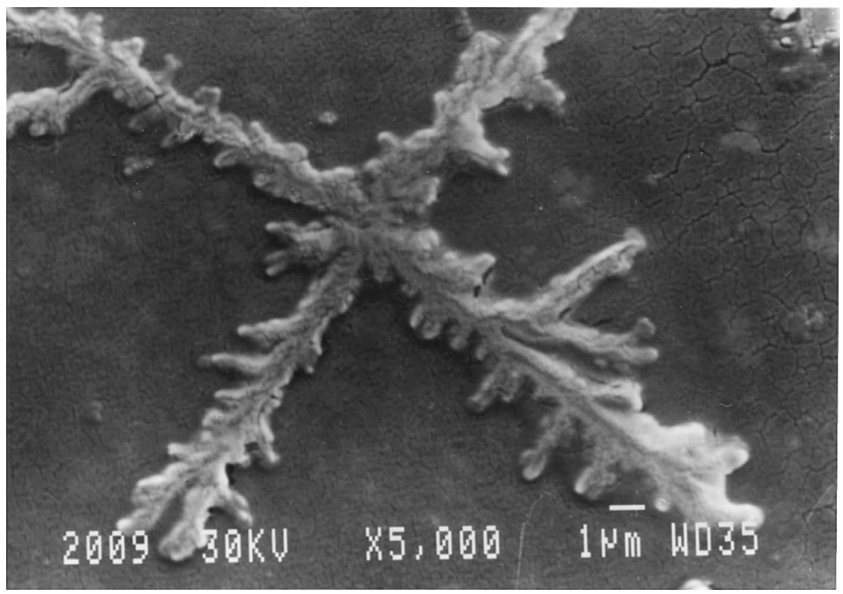

(b)

Figure 8 SEM micrographs for sample with heat treatment: $T_n = 680^\circ$C for $t = 180$ min and $T_c = 900^\circ$C for $t = 15$ min. a) Interior of the sample and b) crystal at higer magnification.

position of lines on Fig. 6 also indicates the change of crystallization mechanism. The change of line slopes occurs only as a result of the dependence of the parameter n on particle sizes, that is, on the mechanism of crystallization.

3.6. Microstructure

Samples prepared for these investigations were compact bulk cylindrical samples, dimensions: diameter 10 mm, length 40 mm. The samples for SEM investigations were prepared perpendicularly and along the axis of the sample and then gold sputtered. On samples which were subjected to heat treatment in two steps: $T_n = 680^\circ$C for $t = 1200$ min and after that $T_c = 950^\circ$C for $t = 30$ min, it was easy to observe on the inside of the samples the equiaxial dendrites with mutual contact. The dendrites have secondary and tertiary fibrils. These investigations established that leucite is grown by the volume crystallization (Fig. 7). X-ray powder pattern of this sample is presented in Fig. 3c. It verifies the fact that the formed crystal phase is a low-temperature modification of leucite with tetragonal symmetry.

In case of samples which were subjected to heat treatment for a short time at crystallization temperature $T = 900^\circ$C (Fig. 8), it is possible to observe dendrites in the volume of the sample undergoing early stage of growth. It is detectable that from the same core four separate crystal arms start to grow. Due to a pronounced anisotropy of the properties such as crystal/glass interfacial energy and growth kinetics, the dendrites grow in preferred crystallographic directions, which are closest

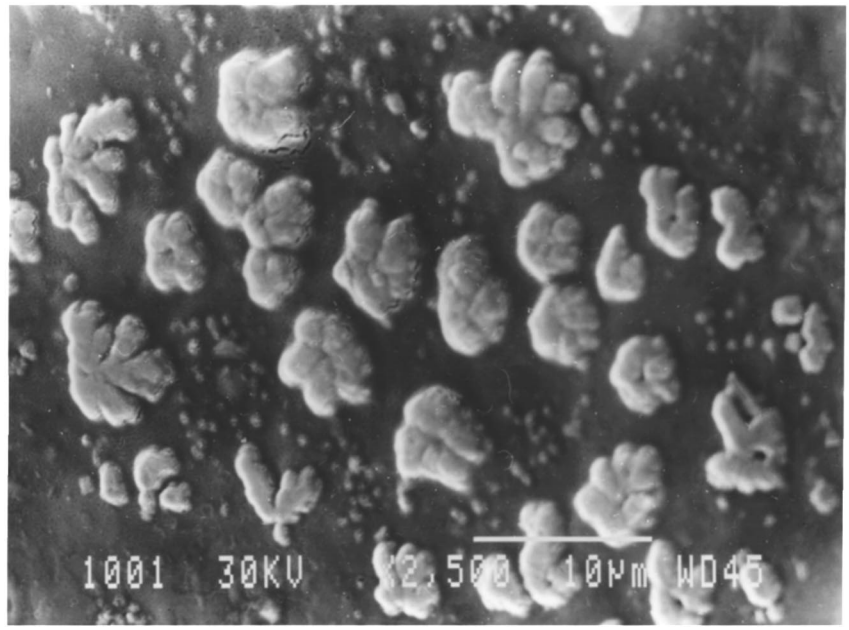

(a)

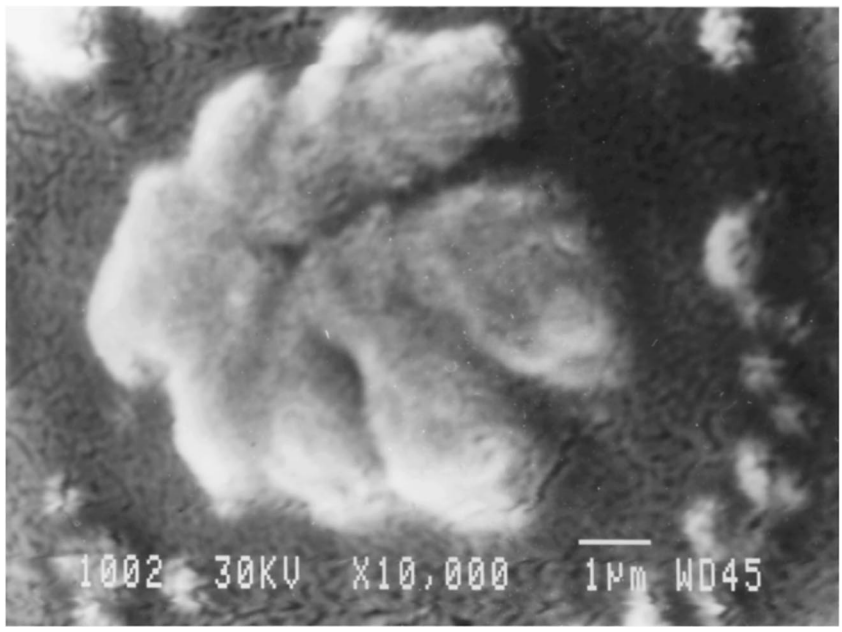

(b)

Figure 9 SEM micrographs for sample with heat treatment: $T_n = 680^\circ$C for $t = 1200$ min and $T_c = 950^\circ$C for $t = 180$ min a) interior of the sample and b) crystal at higer magnification.

to the heat flow. When the heat extraction is isotropic equiaxial dendrites grow along all available preferred directions [22]. In cubic crystals, six directions are available [001]. However, in this investigation it was possible to observe only crystals with fibrils in four directions [001], Fig. 8a, which points to the fact that their growth, in this case, evolves in a thin layer, almost two-dimensionally. Fig. 8b presents the detail of one crystal at higer magnification.

In case of sample which was subjected to heat treatment for a longer period at $T_c = 950^\circ$C, the investigations showed the appearance of thick and deformed dendrites. This indicates that the tops of the fibrils meet the diffusion fields of the neighboring dendrites, so they start ripening and thickening. Therefore the fibrils of the tertiary and higher levels disappear, and their ultimate form easily distinguishable from the initial form (Fig. 9).

4. Conclusion

The subject of the investigation was the crystallization of aluminosilicate glass containing 0.77 wt/% of F^- anion. The dependence of the crystallization mechanism from glass particle sizes has been established. The results of these investigations show that the critical dimension of glass particles for which surface crystallization is switched to volume crystallization is around 0.075 mm. With glass particle sizes dimensioning <0.075 mm, surface crystallization is dominant, while with glass particle sizes dimensioning >0.075 mm, volume crystallization is dominant.

The results of XRD show that in temperature ranges below $T = 950^\circ$C the leucite phase crystallizes. On crystallization temperatures above $T = 950^\circ$C secondary crystal phases of diopside and phlogopite are formed. Rietveld analysis of the sample crystallized at $T = 1000^\circ$C indicate the development of a mixture of crystal phases, containig 58% of leucite, 24% of diopside and 18% of phlogopite.

Investigation of nucleation by DTA method shows that the obtained curve is similar to the nucleation rate curve with, a maximum at a temperature of 680°C, which represents the temperature of maximum nucleation rate T_n. This temperature is higher than the glass transformation temperature T_g.

Kinetic parameters of crystallization show that activation energy of this process is independent from glass crystallization mechanism. The determined value of activation energy is $E_a = 319 \pm 23$ kJ/mol and the Avrami parameter is $n = 1.45$.

The results of investigations of microstructure confirm the development of volume crystallization of leucite in this glass. Leucite crystals grow in form of two-dimensional equiaxial dendrites with pronounced anisotropy along the direction ⟨001⟩. Such morphology of the crystals shows that the process of their growth is controlled by diffusion and that it evolves at the smooth atomic-scale faceted crystal/glass interface. In course of the isothermal heat treatment the structure of dendrites undergoes changes. They grow and reach a highly organized structure with secondary and tertiary fibrils. When the tips of the fibrils meet the diffusion field of the neighboring dendrites, they start ripening and thickening.

References

1. M. H. LEWIS, J. METCALF-JONSEN and P. S. BELL, *J. Amer. Ceram. Soc.* **62** (1979) 277.
2. W. D. KINGERY, H. K. BOWEN and D. R. UHLMANN, "Introduction to Ceramics" (Wiley, New York, 1976).
3. P. W. MC MILLAN, "Non-Metalic Solids: A Series of Monographs No 1. Glass-ceramics," 2nd ed., edited by J. P. Roberts and P. Popper (Academic Press, London, 1979).
4. E. MULLER, H. HEIDE and E. D. ZANOTTO, *Z. f. Kristall.* **200** (1992) 287.
5. R. DIMITRIJEVIC and V. DONDUR, *J. Solid State Chem.* **115** (1995) 214.
6. D. C. PALMER, E. K. H. SALJE and W. W. SCHMAL, *Phys. Chem. Minerals* **16** (1989) 714.
7. S. MUSIC, M. RISTIC, S. POPOVIC, K. FURIC, J. ZIVKO-BANIC and K. MEHULIC, *Mat. Lett.* **27** (1996) 195.
8. W. HOLAND, M. FRANK and V. RHEINBERGER, *J. Non-Cryst. Solids* **180** (1995) 292.
9. W. VOGEL, Glaschemie (VEB Leipzig, 1983).
10. H. M. RIETVELD, *J. Appl. Cryst.* **2** (1969) 65.
11. J. RODRIGUEZ-CARVAJAL, in The XV Congress of the IUCR, Toluse 1990 France, Book of Abstract p. 127.
12. C. S. RAY, Q. YANG, W. HUANG and D. E. DAY, *J. Amer. Ceram. Soc.* **79** (1996) 3155.
13. A. MAROTTA, A. BURI and F. BRANDA, *J. Mater. Sci.* **16** (1981) 341.
14. C. S. RAY and D. E. DAY, *J. Amer. Ceram. Soc.* **73** (1990) 439.
15. E. D. ZANOTTO and M. C. WEINBERG, *Phys. Chem. Glasses* **30** (1989) 186.
16. M. C. WEINBERG, *J. Amer. Ceram. Soc.* **74** (1991) 1905.
17. E. V. SHOKOLNIKOV, *Fiz. khim. stekla* **6** (1977) 153.
18. K. MATUSITA and S. SAKA, *Phys. Chem. Glasses* **20** (1979) 81.
19. K. MATUSITA, T. KOMATU and R. YOKOTA, *J. Mater. Sci.* **19** (1984) 291.
20. T. OZAWA, *Polymer* **12** (1971) 150.
21. D. R. MAC FARLANE and M. FRAGOULIS, *Phys. Chem. Glasses* **27** (1898) 228.
22. K. A. JAKSON, J. D. HUNT, D. R. UHLMANN and T. P. SEWARD, III, *Trans. Met. Soc., AIME* **236** (1966) 149.

Received 18 February 1999
and accepted 17 January 2000